Tellus (1991), *43A*, 334–349

The fractal dimension of drifter trajectories and estimates of horizontal eddy-diffusivity

By BRIAN G. SANDERSON[1] and DAVID A. BOOTH[2], [1]*Department of Physics, Memorial University of Newfoundland, St. John's, NF, A1B 3X7, Canada*; [2]*Maurice Lamontagne Institute, Department of Fisheries and Oceans, 850 route de la Mer, C.P. 1000, Mont Joli, PQ, G5H 3Z4, Canada*

(Manuscript received 21 August 1990; in final form 7 February 1991)

ABSTRACT

We analyze drifter data from the Northeast Atlantic and find that single-particle motion has fractal dimension $D = 1.28 \pm 0.08$ at scales 5 to 100 km. The single particle trajectories are modeled using fractional Brownian motion. Integral time scale is therefore shown to be a function of both the time between position fixes and the length of the total period the drifter was tracked. The variance (particle dispersion) grows as approximately $t^{3/2}$. The probability density function of single-particle velocity is observed to be leptokurtic, consistent with the fractional Brownian motion model. The present work reports two-particle trajectories with fractal dimension $D = 1.3$ for scales from 8 km to 150 km. The two-particle dispersion is modelled as accelerated fractional Brownian motion, in which speed becomes a function of time elapsed since the particles were very near to each other. The acceleration is chosen to be consistent with the patch variance growing as $t^{2.34}$. The dependence of relative velocity between pairs of drifters separated by a distance l, is observed to scale as $l^{0.3}$. This is consistent with the accelerated fractional Brownian motion model for two-particle motion.

1. Introduction

The fractal properties of drifter motion have been investigated recently. Osborne et al. (1986, 1989) studied single-particle motion of drifters drogued at 100 m depth in the Kuroshio extension. They found a fractal dimension $D = 1.27 \pm 0.06$ for scales extending from 20 to 150 km. Sanderson et al. (1990) studied the relative motion between pairs of drifters (two-particle motion) and obtained a fractal dimension of $D = 1.3 \pm 0.1$ for scales extending from 10 to 4000 m.

Fractal drifter trajectories could indicate the presence of chaos due to a low dimension attractor, or alternatively it can result from self-affine stochastic processes (e.g., fractional Brownian motion) as discussed by Osborne and Provenzale (1989). Osborne and Caponio (1990) go further to show how both these types of trajectory can be calculated from a Hamiltonian model for particle motion in two-dimensional turbulence. The Hamiltonian (stream function) was a Fourier series with a spectra consistent with two-dimensional turbulence. Osborne et al. (1991) find that moderate nonlinearity causes the Hamiltonian model to result in particle diffusion over foam-like structures in which case fractal Brownian motion is no longer appropriate. Using a multivariate scaling analysis Osborne et al. (1986) find the drifter trajectories are consistent with stochastic behaviour rather than strange attractors. Osborne et al. (1989) conclude that a first order model of drifter trajectories might be based on additive process, for example fractional Brownian motion. They also found evidence for weak multifractal behaviour, indicative of multiplicative processes. Sanderson et al. (1990) found similar weak multifractal behaviour for relative trajectories. The following work will, therefore, proceed on the basis that single-particle and two-particle motion might, at lowest order, be modeled as fractional Brownian motion (Mandelbrot and Van Ness, 1968; Osborne et al., 1989).

The present work provides additional measurements of the fractal dimension of drifter trajectories. We also measure the magnitude of

Table 1. *Information about each drifter*

Drifter number	Deployment position (lat/long)		Deployment period[†] (Julian Day, Year)	Drogue depth (m)
72	54°49.5′	15°28.9′	137/1983–300/1983	16
73	59°30.1′	9°00.2′	346/1983–155/1984	66
74	59°30.1′	9°1.5′	346/1983–121/1984	16
75	54°49.6′	15°28.9′	137/1983–263/1984	66
76	54°49.8′	15°28.8′	137/1983–343/1983	166
77*	57°21.8′	10°53.0′	25/1984–241/1984	116
78	59°29.5′	8°59.5′	346/1983– 70/1984	116
79	57°31.9′	11°40.5′	25/1984–184/1984	166
80	59°31.7′	8°58.2′	346/1983– 73/1984	116
82	57°31.7′	11°41.8′	25/1984–203/1984	116

[†] The deployment period was deemed to end when a drifter lost its drogue.
* This drifter had an anomalous mean drift.

relative (two-particle) velocity as a function of separation scale. Based on these analyses, the single particle motion is modeled as fractional Brownian motion (Mandelbrot and Van Ness, 1968). The two-particle motion is modeled as an accelerated fractional Brownian motion in which the relative speed between particles increases with the time elapsed since the two particles were infinitesimally near to each other. Using this approach we examine how measurements of eddy-dispersion and integral time/length scales depend upon how the drifter tracking measurements are made. For example, dependence on duration of tracking and time between position fixes will be considered.

In Section 2, we analyse drifter data from the Northeast Atlantic to obtain the fractal dimension of single-particle trajectories. The drifters were released in the Rockall Trough and tracked in the period May 1983 to August 1984. Ten drifters were positioned using ARGOS. They were drogued at depths from 16 m to 166 m. Individual tracks spanned intervals from 3 to 7 months. Table 1 gives basic information about each drifter track. Booth (1988) has estimated horizontal eddy-diffusivities from these data.

In Section 3, we use a fractional Brownian motion model to show how single-particle eddy-diffusivity and integral time scales vary as functions of time between position fixes and total measurement period. The fractional Brownian motion model gives standard deviation of drifter position growing at a rate faster than the classical $t^{1/2}$ dependence found by Taylor (1921) for large t in stationary homogeneous turbulence. Recent analyses that use Taylor's theory, are re-examined from the fractional Brownian motion point of view.

In Section 4, we measure the fractal dimension of two-particle trajectories. This is followed by a reanalysis of data reported by Sanderson et al. (1990), Sanderson (1982), Fahrbach et al. (1986). The data consists of tracks of clusters of drifters in; coastal waters off Long Island, Lake Erie, and in the Atlantic Equatorial Under-current. The relative speed between pairs of drifters is observed to increase with increasing separation scales. Clearly, this will cause relative speed to increase with time, consistent with Okubo (1971). The relative trajectories are therefore modeled as accelerated fractional Brownian motion, where the speed increases with time.

2. Fractal dimension of drifter tracks

We first removed the mean motion of each individual trajectory, in the same manner as Osborne et al. (1989). An algorithm described by Rapaport (1985) was used to obtain trajectory length $L(\eta)$ as a function of "yardstick" length η. Log-log plots of $L(\eta)$ versus η enable calculation of the "divider dimension" D_L which approximates the Hausdorff dimension D. The divider dimension was calculated for each experiment by considering values of η in the range from 5 times the average distance between consecutive points on the trajectory to 0.2 times the maximum distance between

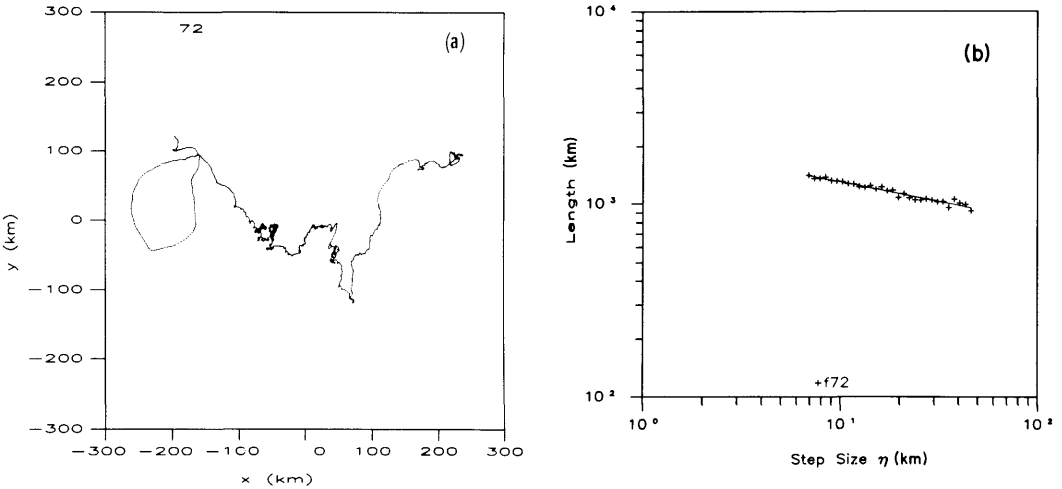

Fig. 1. (a) Trajectory of drifter 72. (b) Log-log plot of trajectory length L as a function of the length of the yardstick η, for the trajectory of drifter 72.

any two points on the trajectory. Both the divider dimension and the range of scales over which it applies are given in Table 2. Fig. 1a shows the trajectory of drifter number 72, and Fig. 1b shows its log-log plot of L versus η. This, and log-log plots for the other drifters are well fitted using straight lines.

There appears to be no obvious dependence of D_L on drogue depth. At the Rockall Trough there is very little stratification in the surface 200 m for the period November to April (Ellet and Martin, 1973). To within experimental error, our average value of $D_L = 1.28 \pm 0.08$ is the same as obtained by Osborne et al. (1989). Our range of scales is 6 km to 100 km, whereas Osborne et al. (1989) covered scales from 20 km to 150 km. This fractal dimension is consistent with two-dimensional turbulence (Osborne et al., 1989; Osborne and Caponio, 1990). Buoy 77 has a larger fractal dimension than the others. It was also observed to have an anomalous mean drift and exhibited considerable eddy activity (Booth and Medrum, 1987).

Table 2. *Fractal dimensions ($\pm$ standard deviation about the regression) of single particle trajectories*

Trajectories number	Divider dimension D_L	Scale range for η (km)
72	1.20 ± 0.01	6.5–42
73	1.29 ± 0.01	7.5–83
74	1.25 ± 0.01	9.5–97
75	1.16 ± 0.01	5.5–35
76	1.18 ± 0.02	7 –88
77	1.40 ± 0.02	7 –55
78	1.26 ± 0.01	10.5–80
79	1.37 ± 0.01	10.5–84
80	1.36 ± 0.02	10 –50
82	1.30 ± 0.02	7.5–63

Average $D_L \pm$ standard deviation of the estimates $= 1.28 \pm 0.08$.

3. Drifter trajectories as fractional brownian motion

It is customary to obain single particle eddy-diffusivities from drifter trajectories by first extracting motion due to some mean current and treating the residual motion $u_i(t) = \partial x_i(t)/\partial t$ as being due to turbulent motion (Freeland et al., 1975; Krauss and Boning, 1987; Garrett et al., 1985; Colin de Verdiere, 1983; Davis, 1985; Thomson et al., 1990). Usually the residual motion is modeled using Taylor's (1921) result that for short time the variance of particle position $x(t_0 + t) - x(t_0)$ grows at t^2, whereas for longer periods it grows proportional to t. Thus the long time behaviour is the same as ordinary Brownian motion

(Mandelbrot and Van Ness, 1968), and is known as the "$t^{1/2}$ law" for the growth of standard deviation.

The results of fractal analysis of trajectories are not consistent with the $t^{1/2}$ law for single particle dispersion. Instead $x(t)$ is more consistent with a fractional Brownian function as discussed by Mandelbrot (1977, 1982). If $x(t)$ is a fractional Brownian function then it is self affine with scaling exponent H, so that

$$[x(t+\Delta t)-x(t)] \stackrel{\mathrm{d}}{=} \lambda^{-H}[x(t+\lambda\,\Delta t)-x(t)], \tag{1}$$

where $\stackrel{\mathrm{d}}{=}$ means equality in the sense of distributions (Osborne et al., 1989). If the drifter motion is isotropic in the x, y plane then $D=\min[1/H, 2]$. The Rockall Trough data are close to isotropic with standard deviations of the x, y components of turbulent velocity being 3.2 cm/s, 4.2 cm/s respectively. Other drifter data sets analysed for single particle dispersion have been even closer to isotropic (Krauss and Boning, 1987; Colin de Verdiere, 1983).

Ordinary Brownian functions have independent Gaussian increments $\mathrm{d}B(t)$ (i.e., the increments are Markovian), whereas increments in fractional Brownian motion have a span of interdependence that is infinite. Fractional Brownian motion with exponent H is a moving average of increments in ordinary Brownian motion $\mathrm{d}B(t)$ in which past increments of ordinary Brownian motion $B(t)$ are weighted by the kernal $(t-s)^{H-1/2}$ as given by (1) in Appendix A, (Mandelbrot and Van Ness, 1968). Following Mandelbrot and Van Ness (1968) we can write a t^{2H} law for single particle dispersion

$$\langle[x(t_0+t)-x(t_0)]^2\rangle = t^{2H}V_H, \tag{2}$$

where

$$V_H=\left[\Gamma\left(H+\frac{1}{2}\right)\right]^{-2}\left\{\int_{-\infty}^{0}[(1-s)^{H-1/2} - (-s)^{H-1/2}]^2\,\mathrm{d}s+\frac{1}{2H}\right\}, \tag{3}$$

and Γ is the gamma function. In (2) the $\langle\ \rangle$ represents an ensemble average, and $x(t)$ is a fractional Brownian function with scaling exponent H. Single particle motion typically has values of $D=1.3$ ($H=1/D=0.77$) and (3) implies, therefore, that variance will grow as time raised to a power of 1.5.

If the power spectrum of trajectories is proportional to frequency raised to a power α then the trajectory dimension is $D=2/(\alpha-1)$ for $1<\alpha<3$ and it is equal to the topological dimension for $\alpha\geqslant 3$ (Osborne and Provenzale, 1989). If $\alpha\geqslant 3$, then we expect the trajectories to be differentiable, and variance of particle dispersion will grow proportional to t^2. The sharp cut off in the power spectrum near the Kolmogorov scale ensures that Taylors (1921) t^2 law holds at these very small scales and that of particle trajectories are differentiable at these small scales. Fractal models of oceanic particle motion can, therefore, only be applicable over a finite range of physical scales. The Kolmogorov microscales are, however, much smaller than the scales of drifter motion considered in this paper. We need not, therefore, observe a t^2 growth of variance at the scales relevant to ocean drifter trajectories.

In Fig. 2a, b we reproduce dispersion curves for the Rockall Trough from Booth (1988). It would appear that a single straight line of slope 1.5 fits the dispersion curve better than dividing the data into t^2 and t regimes. Fig. 2c, d shows the log-log plots of variance versus time from Colin de Verdiere (1983). For the first 10 days, the slopes are approximately 1.5. Certainly the initial slope is much more consistent with a fractal model than with Taylors t^2 law. (The slope for larger t will be discussed later.) Freeland et al. (1975) finds that the initial rate of particle dispersion is overestimated by Taylors theorem, which lends further support to a fractional Brownian motion model. Some of the log-log plots of $\langle[x(t_0+t)-x(t_0)]^2\rangle$ versus time given in Krauss and Boning (1987) appear to be better fitted by a fractal model than by the Taylor t^2 law. Other plots of Krauss and Boning (1987) seem, however, to be well fitted by Taylors t^2 law, but we will show latter how smoothing can result in an initially t^2 law.

At large t the Taylor model reduced to the $t^{1/2}$ law of ordinary Brownian motion and is consistent with a diffusion equation with constant eddy-diffusivity. The distribution of a Gaussian source of scaler tracer, would remain Gaussian. The probability density functions for x and y components of single particle displacements would, therefore, be Gaussian. In Appendix A, we obtain

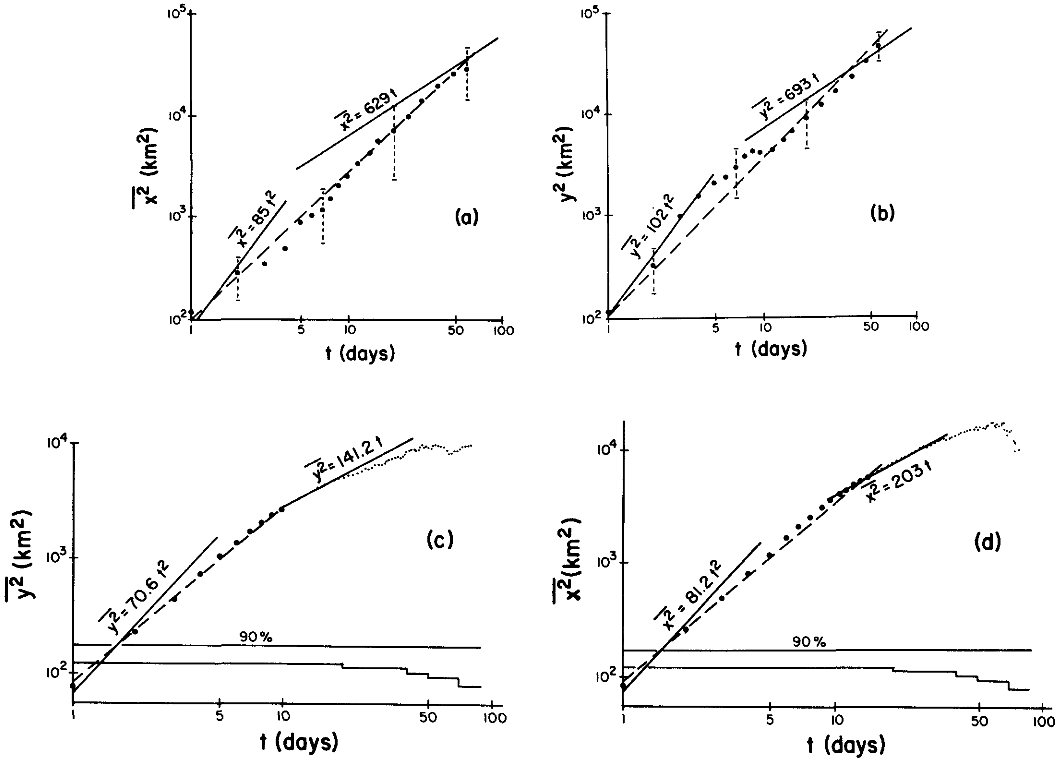

Fig. 2. Booth (1988) obtained the above dispersion curves for the Rockall Trough drifter data: (a) east component, (b) north component. Error bars represent the 5 and 95% fiducial limits. Colin de Verdiere (1983) obtained single particle dispersion curves for trajectories in the eastern North Atlantic: (c) north component, (d) east component. The solid lines represent Taylors small- and large-time approximations. The dashed lines represent 1.5 power law fits, consistent with our measurements of fractal dimension.

an expression for the fourth moment of fractional Brownian motion. Setting the scaling parameter H to $\frac{1}{2}$ we see that the fourth moment is 3 times the square of the second moment. This is consistent with the Gaussian distribution of ordinary Brownian motion. Setting $H=0.75$ we find that the fourth moment is 3.17 times the square of the second moment. This indicates a leptokurtic distribution (Puri and Mulen, 1980). Table 3 shows the ratio of the fourth moment to the square of the second moment for drifter trajectories from the Rockall Trough. A g-test (Geary, 1936) indicates that all of the trajectories have statistically significant leptokurtosis at the 99% confidence level. Table 3 gives values of g for x and y components of motion. It appears that the distribution of particle displacements is even

Table 3. *Ratio of the fourth moment to the square of the second moment for drifter motion; drifter displacements over 2-h periods are considered*

Trajectory number	g_x	g_y	$\frac{\langle x^4 \rangle}{\langle x^2 \rangle^2}$	$\frac{\langle y^4 \rangle}{\langle y^2 \rangle^2}$	Number of displacements
72	0.733	0.733	6.60	4.32	1962
73	0.768	0.782	4.10	3.48	2092
74	0.781	0.761	3.65	3.84	1678
75	0.739	0.653	4.13	7.91	1520
76	0.764	0.743	5.01	6.25	2481
77	0.773	0.761	3.81	4.19	2587
78	0.766	0.781	3.52	3.15	1072
79	0.771	0.785	4.25	3.32	1904
80	0.768	0.780	4.03	3.48	1107
82	0.781	0.762	3.34	3.81	2121

more leptokurtic than expected from a fractional Brownian motion model.

Let us examine the Lagrangian autocorrelation function for fractional Brownian motion. To do this we will consider how the drifter displacement in the period t to $t+\Delta t$ is correlated with the drifter displacement in the period $t+\tau$ to $t+\tau+\Delta t$. Thus we find how the Lagrangian autocorrelation function depends on both the time Δt between position fixes on the drifter and the time lag τ.

$$R_L(\Delta t, \tau) = \frac{\langle [x(t+\Delta t)-x(t)] \times [x(t+\tau+\Delta t)-x(t+\tau)] \rangle}{\langle [x(t+\Delta t)-x(t)]^2 \rangle}. \quad (4)$$

Using the algebraic identity

$$(a-b)(c-d) = \tfrac{1}{2}[(a-d)^2+(c-b)^2 - (a-c)^2-(b-d)^2],$$

and (2), we reduce (4) to

$$R_L(\Delta t, \tau) = \frac{|\Delta t-\tau|^{2H}+(\Delta t+\tau)^{2H}-2\tau^{2H}}{2\Delta t^{2H}}. \quad (5)$$

The Lagrangian autocorrelation is not a function of τ alone. Rather, it becomes a function of the ratio of τ to Δt. As such, the experimental design crucially effects the measurement of the Lagrangian autocorrelation function, and the integral time scales. The Lagrangian autocorrelation is also a function of H, which is the essential characteristic of the dispersive velocity field. A plot of R_L (given by (5) with $H=\frac{3}{4}$) as a function of lag (in units of Δt) is shown by the thin solid line in Fig. 3. Some features of this Lagrangian autocorrelation (obtained from (5)) are similar to measurements of $R_L(\tau)$ obtained from various data sets. For example, it is common to observe a rapid initial decay of R_L for small lags; compare Fig. 3 with Fig. 9 of Colin de Verdiere (1983) and Fig. 3 of Booth (1988). It is common to observe weak correlations for relatively long lags, (e.g., Krauss and Boning, 1987; Colin de Verdiere, 1983; Booth, 1988) however the statistical significance of measured correlations is not always clear for large lags. The autocorrelation sometimes shows evidence of wave-like components of motion, which are not considered in the present fractal approach but could be included in principle.

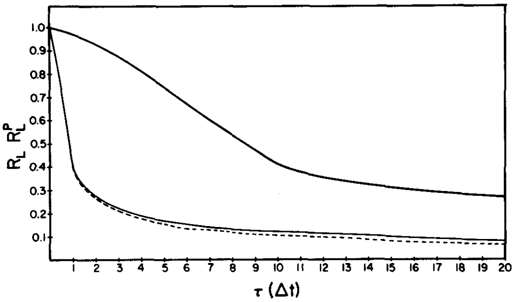

Fig. 3. Dependence of the Lagrangian autocorrelation function upon lag. The thin solid line represents the single particle Lagrangian autocorrelation $R_L(\Delta t, \tau)$ (for fractional Brownian motion as given by (5)) as a function of lag τ expressed in units of Δt. The thick solid line shows the same line with the lag axis expanded to have a factor of 10 more resolution. $R_L^P(t, \Delta t, \tau)$ for accelerated fractional Brownian motion (10) is plotted as a function of lag τ in units of Δt by a dashed line for the case $t=5$ and $\beta=0.4$.

Commonly used methods for defining and extracting the mean Lagrangian motion might partly obscure the true nature of the Lagrangian autocorrelation function of single particle motion. In previous analyses there has been a tendency to define subareas of the total flow field within which the mean flow is homogeneous (e.g., Krauss and Boning, 1987; Poulain and Niiler, 1989). This is justifiable on the small scale, but it does not give a true estimate of absolute (single particle) dispersion since it is really just a way of filtering out the large space scale (long time scale) structure of Lagrangian trajectories. The point is that if we imagine an ocean to consist of areas in which the mean flow is homogenous with areas in between in which the mean flow is inhomogeneous, then it is not correct to simply analyse trajectories in the homogeneous areas in order to determine single particle dispersion. This dispersion is relative to the velocity field of localized subareas and is not global at all. Even if the areas with inhomogeneous mean flow occupy a relatively small portion of the ocean, their effect on dispersing particles is likely to be substantial. Booth and Sephton (personal communication) have observed that there are localized regions in the flow field of a coastal region that play a major role in the overall dispersion of particles. In experiment 3 of Okubo et al. (1983), short bursts of rapid dispersion of a cluster of drifters, occurr infrequently amidst much longer periods of much lesser cluster dispersion. Ottino et al. (1988) examine morphological structures in flow fields and find that some cause regions of rapid mixing, whereas others cause pockets of little mixing.

It makes little formal sense to talk about integral scales for fractal motion which has correlation at all scales. Nevertheless, much of the oceanographic literature interpretes drifter trajectories and eddy-dispersion in terms of integral time scales. We will, therefore, estimate the integral time scales that might be obtained from fractional Brownian drifter trajectories. The integral time scale τ^* is defined as the integral of R_L over a range of lags from 0 to T, where the experiments duration is the upper limit for T:

$$\tau^* = \frac{1}{2\Delta t^{2H}} \int_0^T [(\Delta t - \tau)^{2H} + (\Delta t + \tau)^{2H} - 2\tau^{2H}] \, d\tau$$

$$= \frac{[(\Delta t + T)^{2H+1} + |T - \Delta t|^{2H+1} - 2\Delta t^{2H+1} - 2T^{2H+1}]}{2(2H+1)}. \quad (6)$$

As T tends to infinity, then τ^* tends to infinity also, but in practice the experiments duration is always finite and so is τ^*. The fractional Brownian motion models shows that τ^* is a function of both the measurement interval Δt and the period T over which the experimental measurements span. (Equivalently we could regard this to be a function of the scale of an area that was artificially chosen for analysis in order to ensure homogeneity of the mean flow field.)

The integral time scale for fractional Brownian motion is plotted as a function of T for $H = \frac{3}{4}$ by the dashed line in Fig. 4. Both τ^* and T are expressed in units of Δt. The curve quickly approaches τ^* proportional to $T^{0.49}$. An experiment in which velocities are daily averages (i.e., $\Delta t = 1$ day will give an integral time scale of 2 days if T is 10 days, 7 days for T of 100 days, and 23 days for a T of 1000 days. Thus we see that even for a fractional Brownian motion model it is possible to obtain an integral time scale that is much less than the length of the period over which we measure the particles dispersion. The particle dispersion can, therefore, be approximately modelled on a local scale using Taylor's theory, or equivalently by taking the motion to be Markovian and using a differential diffusion equation with diffusivity chosen in an ad hoc way to represent the time and space scales appropriate for the dispersing tracer distribution. Over sufficiently long periods, however, the correlations between all scales of motion, that characterize fractal trajectories, compel us to choose a new eddy-diffusivity.

Krauss and Boning (1987) obtain average values of $\tau \sim 3$ to 4 days for a T of typically 50, 60 days and $\Delta t = 1$ day averaging of velocity. Several other authors have computed integral time scales of single particle motion, we plot their values of $\tau^*/\Delta t$ versus $T/\Delta t$ in Fig. 4. Values for τ^*, in dimensional units, are given in the caption for Fig. 4. The points on Fig. 4 that are surrounded by dashed boxes are obtained from motion relative to the centroid of a cluster of particles and will be discussed in the next section. For single particle motion, all but one of the points fall within a factor of 3 of the values predicted on the basis of fractional Brownian motion. This scatter might be a result of multifractal aspects of particle motion that increase the variability of statistics from that expected on the basis of fractional Brownian motion. Osborne and Caponio (1990) observe that particle diffusion occurs over foamlike structures when particle trajectories are calculated from a moderately nonlinear flow field. This indicates multifractallity.

The single particle data are somewhat scattered on Fig. 4. Nevertheless it is well to note that our fractal interpretation greatly reduces the variability observed for single particle integral time scales. For example, consider the integral time scales of Garrett et al. (1985) which are typically 15 hours, whereas those of Freeland et al. (1975) are 10 to 12 days. This is a difference by a factor of about 20, however when we plot these integral time scales on Fig. 4 we see that their real difference (in terms of distance from the dashed line) is only a factor of about 2. Differences in τ^* are sometimes more due to differences in measurement technique than nature.

Poulain and Niiler (1989) find that the integral

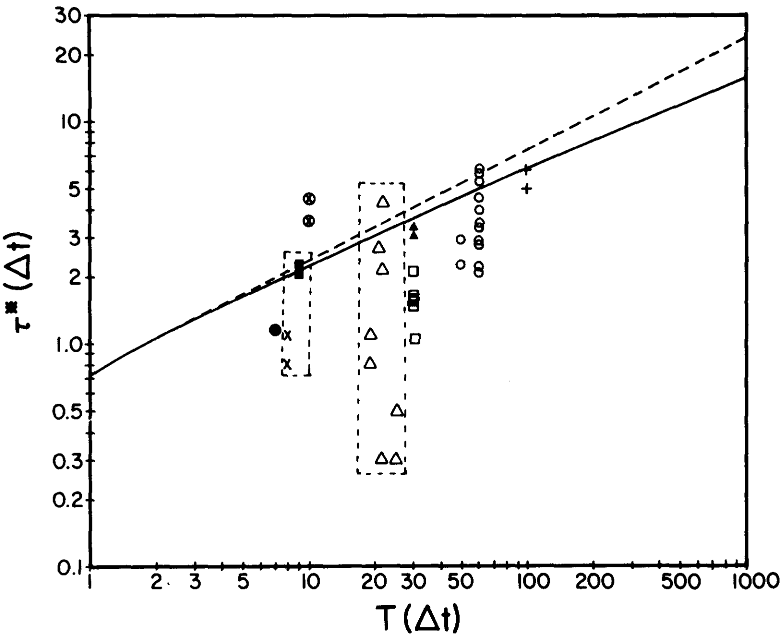

Fig. 4. Log-log plot of integral time scale τ^* versus integration period T. Both T and τ are expressed in units of the measurement interval Δt. The dashed line is for fractional Brownian motion with scaling parameter $H = \frac{4}{3}$. The solid line is for accelerated fractional Brownian motion, with $\beta = 0.4$. The symbols represent experimentally determined integral time scale τ^* versus the period the Lagrangian autocorrelation is integrated over T. Points obtained from cluster experiments are surounded by dashed boxes. All other points are obtained from single particle statistics. Points are obtained from:

■ LEDS Winter cluster experiments; $\tau^* = 41.7$ and 43.8 min; Sanderson (1982), Pal (personal communication).
× LEDS Summer cluster experiments; $\tau^* = 10.0$ and 13.5 min; Sanderson (1982), Pal (personal communication).
△ Atlantic Equatorial Under Current cluster experiments; $\tau^* = 17$, 18, 31, 50, 67, 132, 160, 254 min; Sanderson and Pal (1990).
○ Atlantic single-particle trajectories; $\tau^* = 4.5$, 5.6, 8.6, 5.9, 6.0, 3.4, 3.0, 2.3, 2.8, 3.2, 2.1, 2.1, 3.2, 2.2, 4.0, 2.9 days; Krauss and Boning (1987).
□ Iceberg trajectories (single particle motion); $\tau^* = 10$, 16, 17, 17, 15, 21 h; Garrett et al. (1985).
+ 1500 m deep single particle trajectories at the MODE site; $\tau^* = 10.1$, 12.3 days; Freeland et al. (1976).
● Single particle trajectories in CODE; $\tau^* = 1.5$ days; Davis (1985).
⊗ Single particle trajectories in the north Pacific; $\tau^* = 4.5$, 3.6 days; Thomson et al. (1990).
▲ Single particle trajectories in the eastern north Atlantic; $\tau^* = 3.1$, 3.4 days; Booth (1988).

of the drifter velocity autocovariance does not approach a constant limit at T is increased. This is consistent with a fractional Brownian motion model. It is common (Poulain and Niiler, 1989; Davis, 1985) to simply integrate up to the first zero crossing to obtain integral time scales. This obviously gives valuable information about the time scale for cyclic wave or eddy motion. However it gives very limited information about particle dispersion, because an integral scale estimated in this manner is only useful for calculating dispersion over time periods up to the time of the zero crossing.

One disconcerting property of fractional and ordinary Brownian motion is that it is not differentiable. This property may not be very limiting, however, since velocity measurements are always integrated versions of a quantity that has variability at all scales down to the Kolmogorov scales (as discussed earlier). Mandelbrot and Van Ness (1968) show that smoothing can make the fractional Brownian motion differentiable. For example a kernel ψ can be used to obtain a smoothed fractional Brownian motion $x_s(t)$, that is differentiable, from a discontinuous fractional Brownian motion $x(t)$.

$$x_s(t; s) = \int_{-\infty}^{\infty} x(s)\,\psi(t-s)\,\mathrm{d}s. \tag{7}$$

In Appendix B we show that applying the smoothing kernel of ψ to recast $x(t)$ as a smoothed fractional Brownian motion enables us to rewrite (2) as

$$\begin{aligned}\langle [x_s(t)-x_s(0)]^2 \rangle &= \int_{-\infty}^{\infty} \psi(q) \int_{-\infty}^{\infty} \psi(q+r)\, V_H[|t-r|^{2H} \\ &\quad + |t+r|^{2h} - 2\,|r|^{2H}]\,\mathrm{d}r\,\mathrm{d}q. \end{aligned} \tag{8}$$

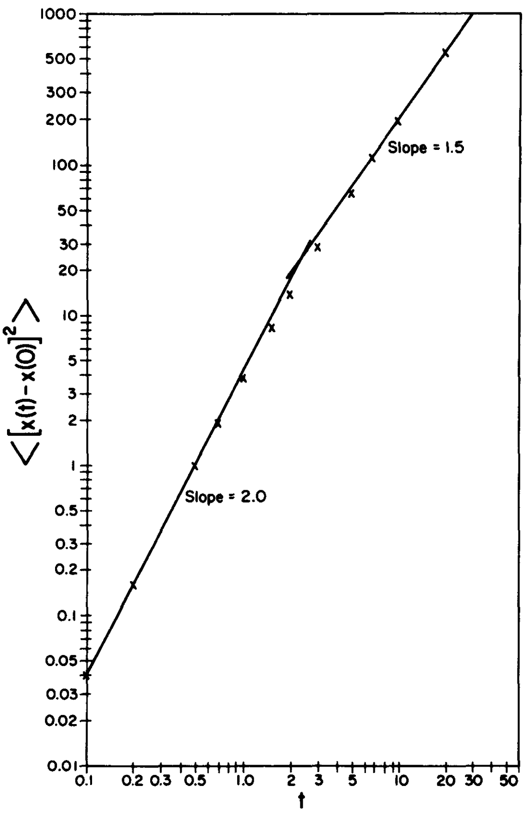

Fig. 5. Plot of variance versus time for smoothed fractional Brownian motion. The smoothing kernel is $\psi = \pi^{0.5} e^{-q^2}$.

Taking ψ to be a Gaussian function $\psi(q) = \pi^{-0.5} e^{-q^2}$ we plot variance versus time in Fig. 5. For $t \ll 2$ we find that variance increases proportional to t^2, whereas for $t \gg 2$ it increases as t^{2H}. Judicious application of these assymptotic forms for the dependence of variance on t gives the variance for the full range of t to within a 10% error. The lack of a t^2 regime in Fig. 2 indicates that smoothing is not required to within the temporal resolution of the data. It also follows that smoothing of data can artificially cause a t^2 rate of growth of variance for small t.

In summary, there is evidence that single particle dispersion is fractal for scales spanning 6 km to 150 km. Thus concepts such as integral time scales become a function of the record length and time interval between position fixes. The Lagrangian autocorrelation functions and single particle dispersion measured by Krauss and Boning (1987) are sometimes more like Taylor's model and at other times more consistent with the fractal model. It should be noted, however, that Krauss and Boning (1987) divided their data regionally (into homogeneous subareas) and truncated it temporally, in such a way that its fractal properties would be "filtered out" and it would be constrained to approximately fit the Taylor (1921) model. Similarly removing the mean velocity of each drifter (Poulin and Niiler, 1989; and the present paper) removes current variability at scales comparable to the time series/trajectory length. This is one of several reasons why the present work only considers yardsticks smaller than 0.2 times the scale of the trajectory with the mean motion removed. It is not, therefore, of any great significance that for large t the rate of growth of variance calculated by Krauss and Boning (1987), Colin de Verdiere (1983), and Poulain and Niiler (1989) is sometimes inconsistent with fractional Brownian motion, since this could be more an artifact of data analysis techniques than of nature.

4. An accelerated fractal model for two particle dispersion

Sanderson et al. (1990) have results indicating that the trajectory of one drifter relative to another (two-particle trajectory) has a fractal dimension of about 1.34 ± 0.12 over scales from 10 m to 4000 m. Our present data set yields one relative trajectory for much larger separation scales. Drifters 77 and 82 were released near each other at almost the same time and were both drogued at 166 m. The relative trajectory of 77 and 82 is plotted in Fig. 6. The divider dimension of their relative trajectory is 1.36 and spans a range of scales from 8 km to 150 km. This divider dimension was calculated in exactly the same manner as used by Sanderson et al. (1990) to calculate divider dimensions.

The following pairs of drifters were released at similar places at similar times, however, they had drogues set at different depths. The relative trajectories of drifters 73–74, 74–78, 79–82, and 78–80 were analyzed to find their divider dimension. Considering all these two-particle trajectories gives an average fractal dimension 1.28 ± 0.08.

It is reasonable to expect that single particle motion is stationary in the sense that the ensemble average of particle speed is not a function of time. Ever greater dimension eddies contribute to relative motion as the drifters spread apart. Thus the ensemble average of the relative speed between particles becomes a function of their separation scale. In Fig. 7 we plot a regression line of relative speed as a function of separation distance for all drifter pairs within each of the following drifter cluster experiments that have been reported previously by Sanderson and Pal (1990), Sanderson (1982), and Fahrbach et al. (1986). To avoid blacking out Fig. 7, we plot only every third point.

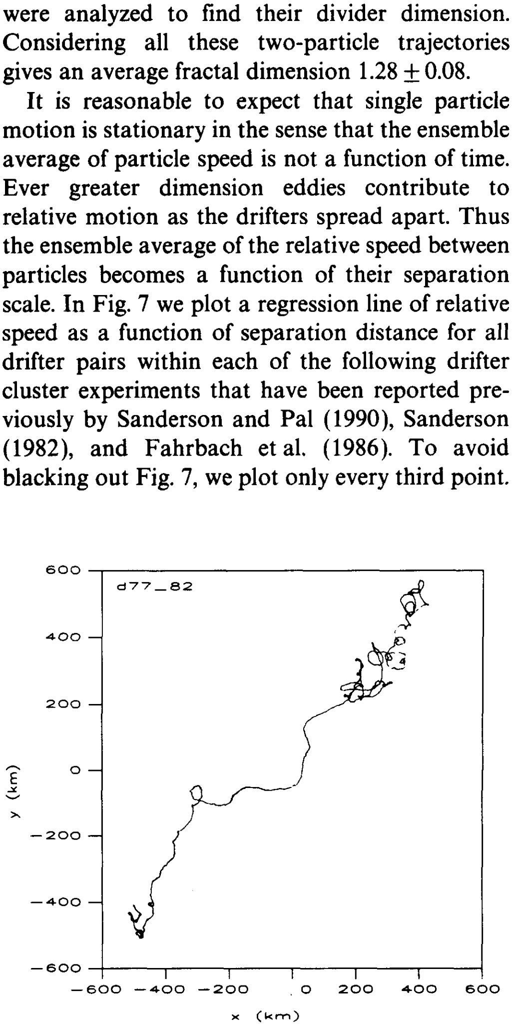

Fig. 6. The two-particle trajectory of drifter 77 relative to 82.

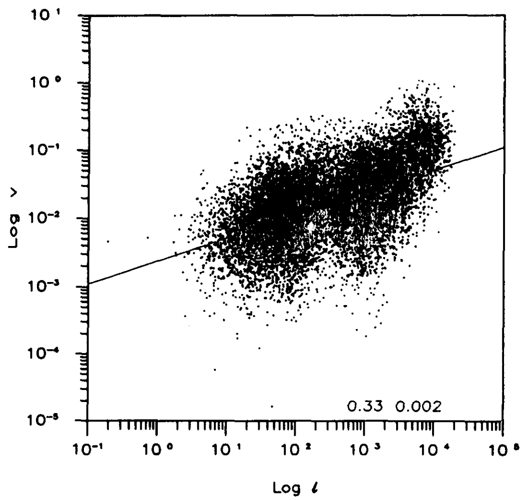

Fig. 7. Log of relative speed between two drifters versus log of relative separation distance between drifters. Data are obtained from drifter cluster experiments in Lake Erie, off the south shore of Long Island, and in the Atlantic Equatorial undercurrent. Only every third point is plotted. The best fit regression has a slope 0.33.

Lake Erie drifter cluster experiments consist of 8387 drifter positions; LEDS winter/summer experiments consist of 1740/1846 drifter positions off the south shore of Long Island; Atlantic Equatorial undercurrent cluster experiments consist of 2533 drifter positions. There is a great deal of scatter in the magnitudes of relative speed as a function of separation. Such scatter is not altogether surprising for individual samples from a "coloured" random noise, especially if we consider that it may be somewhat multifractal as discussed earlier. Nevertheless, there is a general trend for the relative speed to increase as distance of seperation raised to a power of 0.33. When the same analysis is done for individual groups of data, then a similar dependence on separation scale is observed (Table 4). This dependence of relative velocity upon separation scale results in variance of patches growing faster than t^2. Okubo (1971) finds that patch variance grows as $t^{2.34}$. Patch dispersion and two particle dispersion, within a patch, differ only by a factor of 2 (Batchelor, 1952; Brier, 1959), so a $t^{2.34}$ law should also hold for the rate of increase of mean square separation of pairs of particles. This is much faster than the t^{2H} of fractional Brownian motion.

Table 4. *The dependence of relative speeds of pairs of particles upon the separation distance l*

Experiments	Power dependence
Leds Summer data Sanderson et al. (1990)	0.26
Leds Winter data Sanderson et al. (1990)	0.34
Lake Erie data Sanderson et al. (1990)	0.22
Equatorial data Sanderson and Pal (1990) Fahrbach et al. (1986)	0.24
Regression for all data	0.33

Let us denote the relative displacement between a pair of drifters by $x_p(t)$ at time t. In this case we can model $x_p(t)$ as fractional Brownian motion that is a function of a rescaled variable t', and which has a scaling parameter H,

$$x_p(t) = \frac{1}{\Gamma[H+\frac{1}{2}]} \int_{-\infty}^{0} [(t'-s)^{H-1/2} - (-s)^{H-1/2}] \, dB(s) + \int_0^{t'} (t'-s)^{H-1/2} \, dB(s),$$

where $t' = t^\beta$ and $B(s)$ is ordinary Brownian motion. The time t must now be referenced to an initial time $t=0$ when the relative distance between particles tends to zero. The rescaling of time will still give trajectories on the x, y plane that have scaling parameter H. However, the relative speed along the trajectory will not be stationary, rather it will accelerate. The mean square particle separation will therefore grow as

$$\langle x_p^2 \rangle = t^{2H+\beta} V_H. \tag{9}$$

Given that $H = 1/D_f = 1/1.3$, it seems that $\beta \simeq 2.34 - 1.54 = 0.8$ to be consistent with the patch dispersion observations of Okubo (1971). This means that the relative speed between particles scales as $t^{\beta/2} = t^{0.4}$. This dependence of relative speed on time is also consistent with our earlier independent observation that the relative speed between particles $d\,|x_p|/dt$ is proportional to separation to a power of 0.3; i.e., $|x_p|^{0.3}$. This can be seen by solving

$$\frac{d\,|x_p|}{dt} \sim |x_p|^{0.3}$$

for $|x_p|$ as a function of t and differentiating with respect to t to obtain

$$\frac{d\,|x_p|}{dt} \sim t^{0.4} = t^{\beta/2}.$$

A Taylor model of dispersion gives variance growing as t, for large t. Considering the memory of the trajectory gives a fractional Brownian motion that results in variance growing as $t^{1.5}$. Considering that the speed increases with increasing separation scale, we see that an accelerated fractional Brownian motion model gives variance growing as $t^{2.34}$, consistent with Okubo (1971). The rate of growth of two-particle variance is rapid compared to Taylors (1921) model. This is partly due to the non-Markovian nature of the trajectory, but it is mostly due to the relative speed increasing with separation scale.

To examine the temporal correlations of such a flow we proceed as for the derivation of (5), but rescale the time variable so that

$$\begin{aligned} R_L^p(t, \tau, \Delta t) = \{ & [(t+\Delta t)^\beta - (t+\tau)^\beta]^{2H} \\ & + [(t+\Delta t+\tau)^\beta - t^\beta]^{2H} - [(t+\Delta t)^\beta \\ & - (t+\Delta t+\tau)^\beta]^{2H} - [t^\beta - (t+\tau)^\beta]^{2H} \} \\ & /\{2[(t+\Delta t)^\beta - t^\beta]^{2H}\}. \end{aligned} \tag{10}$$

Note that R_L^p is a function of time since the start of the experiment, which is taken as the time $t=0$ when the two particles started from the same point source. The shape of this autocorrelation function is plotted on Fig. 3 for $\Delta t = 1$, and $t = 5$. The correlations drop off a little quickly for the accelerated fractional Brownian motion, than they do for the fractional Brownian motion. In the limit $t \gg \tau, \Delta t$ we find that R_L^p becomes R_L as given by (5). Thus if we make Δt sufficiently small we see that locally (i.e., for small changes in t) there is much in common between two-particle dispersion and single particle dispersion.

The two-particle integral time scale found by integrating (10) up to some time T is plotted with a solid line on Fig. 4. The two-particle integral time scale increases as $T^{0.41}$ for accelerated fractional Brownian motion with $\beta = 0.8$, $H = 0.75$. The ratio of two-particle integral time scale to measurement period falls off proportional to $T^{-0.59}$. The integral scales of accelerated fractional Brownian motion therefore become small compared to patch time and space scales at a rate that is a little more rapid than for fractional Brownian motion. Considering the dispersion as a function of time we see that after 40 measurement intervals the integral time scale becomes less than $\frac{1}{10}$ of the measurement period. Thus for most of the experiment the integral length/time scales are much less than the patch space scales and time over which diffusion has taken place. It is little wonder therefore that a differential diffusion equation with eddy-diffusivities chosen to be appropriate for the patch scale, can give a reasonable description of patch dispersion. However if we are to consider patch dispersion over long periods of time it clearly becomes necessary to make the integral time scale τ^*, relative turbulent velocity, and eddy-diffusivity, all functions of time.

The dependence of integral time scale τ^* on T and Δt can be illustrated from drifter experiments that have been previously analyzed. This is very much the case as can be seen from plotting (in Fig. 4) $\tau^*/\Delta t$ versus $T/\Delta t$ for relative drifter motion obtained from LEDS summer, LEDS winter, and Atlantic Equatorial Undercurrent data with crosses, solid boxes, and triangles respectively. The points fall close to where they would if they were due to single particle motion. On Fig. 4, the integral time scales obtained by Thomson et al. (1990) (plotted by a cross inside a circle) for single particle motion with $\tau = 4.5, 3.6$ days, $T = 10$ days and $\Delta t = 1$ day fall very close to the two-particle integral time scales obtained from the winter LEDS data in which $\tau = 41.7, 43.8$ minutes, $T = 170$ min and $\Delta t = 10$ min. This suggests that integral time scale is as much a function of experimental design and methods of data processing, as it is of the properties of the flow field. Integral scales from the Atlantic Equatorial Undercurrent (Sanderson and Pal, 1990) comply least with the fractional Brownian motion model. Nevertheless their relative trajectories are fractal with dimension 1.3 (Sanderson et al., 1990).

The relatively large scatter observed in Fig. 4 for the Atlantic Equatorial Undercurrent data can be in part attributed to the relatively small number of measurements (compared to the LEDS data) used to obtain each of the integral time scales plotted (Sanderson and Pal, 1990). Sanderson et al. (1990) also found evidence for weak multifractality, that could also limit the fractal Brownian motion model to only being accurate at lowest order. The fractional Brownian motion considered here, does not have a wave component to the motion. This might be a weakness for modelling the integral time scales in some of the wavy environments, such as the Atlantic Equatorial Undercurrent (Sanderson and Pal, 1990).

5. Summary

We have presented further evidence that single particle drifter trajectories have fractal dimension of about 1.3. A first approach to modelling such trajectories might, therefore, be as fractional Brownian motion. The fractional Brownian motion model results in dispersion growing with time in a manner that often fits observations better than the usually applied Taylor model. The Lagrangian autocorrelation function for fractional Brownian motion falls off rapidly for small lags. This is consistent with observations, and explains the lack of a t^2 growth of variance. An initial t^2 growth of variance can be forced by smoothing, but this does not seem appropriate for the scales of presently available data sets. An integral time scale was calculated by integrating the Lagrangian autocorrelation function. The integral time scale (and hence diffusivity) is a function of the fractal dimension, the time between independent observations of drifter positions, and the time interval over which the Lagrangian autocorrelation function is integrated. This also shows that the time (and space) scales averaged over in order to extract the mean motion, must be much greater than the time (and space) scales that we are calculating dispersion over. This latter point is crucial to the proper interpretation of drifter observations.

Relative trajectories are also observd to have fractal dimension of 1.3 over a wide range of scales. The rate of growth of variance of relative position is, however, faster than can be accounted for by fractional Brownian motion. We propose, therefore, that relative motion can be modelled using an accelerated fractional Brownian motion model. This model considers a rescaling of time so that the relative speed increases with time, consistent with the dispersive action of ever larger eddies as the patch spreads. Measurements confirm that relative speed between particles increases as the particle separation increases.

The fractal properties of drifter motion result in it being fundamentally non-Markovian, therefore differential diffusion equations are, in principle, inappropriate for relative dispersion. This point has been noted by others (Davis 1983). Nevertheless the fractional Brownian motion model shows that the Lagrangian autocorrelation function falls off sufficiently fast so that both the relative and absolute motion soon become substantially decorrelated as noted in the above discussion of integral time scales. It follows that differential diffusion equations are approximately applicable for both absolute and relative drifter dispersion. The diffusivities will, of course, have to be functions of time. It is interesting that integral time scales are smaller for relative motion than for single particle motion (Fig. 4). This implies that the Markovian assumption results in less error for modelling relative dispersion than it does for single particle dispersion.

Work by Osborne and Caponio (1990), Osborne and Provenzale (1989), Osborne et al. (1991) clearly indicates the possibility that drifter trajectories are multifractal. If this is the case, then the present work should be viewed as a lowest-order model for drifter dispersion. Previous data analyses (Osborne et al., 1989; Sanderson et al., 1990) suggest that drifter motion has weak multifractallity.

6. Acknowledgement

We thank Dr. A. R. Osborne and an anonymous reviewer for helpful comments.

7. Appendix A

Let ordinary Brownian motion be represented by $B(t)$ which is a real random function with independent Gaussian increments. Following Mandelbrot and Van Ness (1968) we represent fractional Brownian motion with scaling exponent H by $B_H(t)$ which is obtained from $B(t)$ using a weighting kernel as follows.

$$B_H(t)-B_H(O)=\frac{1}{\Gamma(H+\frac{1}{2})}\times\left\{\int_{-\infty}^{0}[(t-s)^{H-1/2}-(-s)^{H-1/2}]\,\mathrm{d}B(s)+\int_0^t (t-s)^{H-1/2}\,\mathrm{d}B(s)\right\}. \tag{A-1}$$

Since

$$\langle[B_H(t_0+t)-B_H(t_0)]^4\rangle=\langle[B_H(t)-B_H(O)]^4\rangle, \tag{A-2}$$

it follows that

$$\langle[B_H(t_0+t)-B_H(t_0)]^4\rangle=\frac{1}{[\Gamma(H+\frac{1}{2})]^4}\times\left\langle\left\{\int_0^t (t-s)^{H-1/2}\,\mathrm{d}B(s)+\int_{-\infty}^{0}[(t-s)^{H-1/2}-(-s)^{H-1/2}]\,\mathrm{d}B(s)\right\}^4\right\rangle. \tag{A-3}$$

Recognizing the independence of the two integrals enclosed in brackets on the right hand side of [A-3] we obtain

$$\langle[B_H(t_0+t)-B_H(t_0)]^4\rangle=\frac{1}{[\Gamma(H+\frac{1}{2})]^4}\times\left\{3\left[\int_0^t (t-s)^{2H-1}\,\mathrm{d}s\right]^2+3\left[\int_{-\infty}^{0}[(t-s)^{H-1/2}-(-s)^{H-1/2}]^2\,\mathrm{d}s\right]^2+2\int_0^t (t-s)^{2H-1}\,\mathrm{d}s\int_{-\infty}^{0}[(t-s)^{H-1/2}-(-s)^{H-1/2}]^2\,\mathrm{d}s\right\}, \tag{A-4}$$

where we have used

$$\langle \mathrm{d}B(s)\,\mathrm{d}B(r)\rangle=\begin{cases}\mathrm{d}s & \text{if } r=s\\ 0 & \text{if } r\neq s.\end{cases} \tag{A-5}$$

A change of variables $s = ts'$ gives:

$$\langle [B_H(t_0+t) - B_H(t_0)]^4 \rangle = \frac{t^{4H}}{[\Gamma(H+\frac{1}{2})]^4} \times \left\{ 3\left[\int_{-\infty}^{0} [(1-s)^{H-1/2} - (-s)^{H-1/2}]^2 \, ds\right]^2 + \frac{3}{(2H)^2} + \frac{1}{H}\int_{-\infty}^{0} [(1-s)^{H-1/2} - (-s)^{H-1/2}]^2 \, ds \right\}, \tag{A-6}$$

where we have dropped the prime in [A-6]. In the limit $H = \frac{1}{2}$, [A-6] reduces to

$$\langle [B_{1/2}(t_0+t) - B_{1/2}(t_0)]^4 \rangle = 3t^2 = 3\langle [B_{1/2}(t_0+t) - B_{1/2}(t_0)]^2 \rangle^2. \tag{A-7}$$

This is the usual relationship for a Gaussian distribution.

8. Appendix B

Smoothed fractional Brownian motion $B_H^S(t)$ can be written as the following function of fractional Brownian motion $B_H(t)$ and a weighting kernel ψ

$$B_H^S(t) = \int_{-\infty}^{\infty} B_H(s)\,\psi(t-s)\,ds, \tag{B-1}$$

where

$$\int_{-\infty}^{\infty} \psi(q)\,dq = 1, \tag{B-2}$$

or under the transform $q = s - t$:

$$B_H^S(t) = \int_{-\infty}^{\infty} B_H(t+q)\,\psi(q)\,dq,$$

if ψ is an even function; $\psi(+q) = \psi(-q)$.

$$B_H^S(t+t_0) - B_H^S(t_0) = \int_{-\infty}^{\infty} \psi(q)[B_H(t+t_0+q) - B_H(t_0+q)]\,dq = \int_{-\infty}^{\infty} \psi(q)[B_H(t+q) - B_H(q)]\,dq. \tag{B-3}$$

Now the ensemble average is not a function of q, so we can take it inside the integral over all q space:

$$\langle [B_H^S(t+t_0) - B_H^S(t_0)]^2 \rangle = \int_{-\infty}^{\infty}\int_{-\infty}^{\infty} \psi(q')\,\psi(q) \times \langle [B_H(t+q) - B_H(q)][B_H(t+q') - B_H(q')] \rangle \,dq\,dq'. \tag{B-4}$$

Now, if $q' = q + r \Rightarrow dq' = dr$, then

$$\langle [B_H^S(t+t_0) - B_H^S(t_0)]^2 \rangle = \int_{-\infty}^{\infty}\int_{-\infty}^{\infty} \psi(q+r)\,\psi(q) \times \langle [B_H(t+q) - B_H(q)][B_H(t+q+r) - B_H(q+r)] \rangle \,dr\,dq. \tag{B-5}$$

Using the relation

$$(a-b)(c-d) = \tfrac{1}{2}[(a-d)^2 + (c-b)^2 - (a-c)^2 - (b-d)^2],$$

the above integral reduces to

$$\int_{-\infty}^{\infty}\int_{-\infty}^{\infty} \psi(q+r)\,\psi(q) \times \langle [B_H(t+q) - B_H(q+r)]^2 + [B_H(t+q+r) - B_H(q)]^2 - [B_H(t+q) - B_H(t+q+r)]^2 - [B_H(q) - B_H(q+r)]^2 \rangle \,dr\,dq. \tag{B-6}$$

This reduces to

$$\langle [B_H^S(t+t_0) - B_H^S(t_0)]^2 \rangle = \int_{-\infty}^{\infty}\int_{-\infty}^{\infty} \psi(q+r)\,\psi(q)\,V_H \times [|t-r|^{2H} + |t+r|^{2H} - 2\,|r|^{2H}]\,dr\,dq, \tag{B-7}$$

where V_H is given by (3) in the main text. In the limit that t is much greater than the values of r such that $\psi(r) \to 0$, we see that [B-7] reduces immediately to

$$\langle [B_H^S(t+t_0) - B_H^S(t_0)]^2 \rangle = t^{2H} V_H, \tag{B-8}$$

for large r, which is the identical result expressed by (2) for dispersion by fractional Brownian motion.

The limit that t is much smaller than the width of the weighting kernel gives

$$\langle [B_H^S(t+t_0) - B_H^S(t_0)]^2 \rangle$$

$$= t^2 V_H 2H(2H-1) \int_{-\infty}^{\infty} \psi(q)$$

$$\times \int_{-\infty}^{\infty} \psi(q+r)\, r^{(2H-2)}\, \mathrm{d}r\, \mathrm{d}q + O(t^4), \qquad \text{(B–9)}$$

which increases at t^2, just like the small time behaviour considered by Taylor (1921). For $H = \frac{1}{2}$ the small time limit gives zero dispersion, as it must since the smoothed displacements become the average of many independent random numbers in this instance.

Let us take a smoothly varying kernel function that is infinitely differentiable and symmetric

$$\psi(q) = \frac{1}{\sqrt{\pi}} e^{-q^2}, \qquad \text{(B–10)}$$

and satisfies the normality condition when integrated over all space. Substituting [B–10] into [B–7] and integrating numerically gives the plot shown in Fig. 5.

REFERENCES

Batchelor, G. K. 1952. Diffusion in a field of homogeneous turbulence. II. The relative motion of particles. *Proc. Camb. Phil. Soc. 48*, 345–362.

Booth, D. A. 1988. Horizontal dispersion in the northeast Atlantic. *Deep-Sea Research 35*, 1937–1951.

Booth, D. A. and Meldrum, D. T. 1987. Drifting buoys in the Northeast Atlantic. *J. Cons. int. Explor. Mer. 43*, 261–267.

Brier, G. W. 1959. The statistical theory of turbulence and the problem of diffusion in the atmosphere. *J. Met. 7*, 283.

Colin de Verdiere, A. 1983. Lagrangian Eddy Statistics from Surface Drifters in the Eastern North Atlantic. *J. Mar. Res. 41*, 375–398.

Davis, R. E. 1985. Drifter Observations of Coastal Surface Currents During CODE: The Statistical and Dynamical Views. *J. Geophys. Res. 90*, 4756–4772.

Davis, R. E. 1983. Oceanic property transport, Lagrangian particle statistics and their prediction, *J. Mar. Res. 41*, 164–194.

Ellet, D. J. and Martin, J. H. A. 1973. The physical and chemical oceanography of the Rockall Channel. *Deep-Sea Research 20*, 585–625.

Fahrbach, E., Brockmann, C. and Meincke, J. 1986. Horizontal mixing in the atlantic equatorial undercurrent estimated from drifting buoy clusters. *J. Geophys. Res. 91 (C9)*, 10557–10565.

Freeland, H. J., Rhines, P. B. and Rossby, T. 1975. Statistical observations of the trajectories of neutrally buoyant floats in the North Atlantic. *J. Mar. Res. 33*, 383–404.

Garrett, C., Middleton, J. F., Majaess, F. and Hazen, M. 1985. *Analysis and prediction of iceberg trajectories.* Department of Oceanography, Dalhousie University, Nova Scotia, 86 pp.

Geary, R. C. 1936. Moments of the ratio of the mean deviation to the standard deviation for normal samples. *Biometrika 28*, 295–307.

Krauss, W. and Boning, C. W. 1987. Lagrangian properties of eddy fields in the northern North Atlantic as deduced from satellite-tracked buoys. *J. Mar. Res. 45*, 259–291.

Mandelbrot, B. B. 1977. *Fractals: form, chance and dimension.* W. H. Freeman and company, San Francisco, 365 pp.

Mandelbrot, B. B. 1982. *The fractal geometry of nature.* W. H. Freeman and Company, New York, 468 pp.

Mandelbrot, B. B. and Van Ness, J. W. 1968. Fractional Brownian motions, fractional noises and applications. *SIAM Review 10*, 422–437.

Okubo, A. 1971. Oceanic diffusion diagrams. *Deep-Sea Research 18*, 789–806.

Okubo, A., Carter, H. H., Wilson, R. E., Sanderson, B. G. and Partch, E. N. 1983. *A Lagrangian Eulerian diffusion study in the coastal surface layers.* Special Report 46, Reference 83–1, Marine Sciences Research Center, SUNY, 295 pp.

Osborne, A. R. and Caponio, R. 1990. Fractal trajectories and anomalous diffusion for chaotic particle motions in 2D turbulence. *Phys. Rev. Lett. 64*, 1733–1736.

Osborne, A. R., Caponio, R. and Pastorello, A. 1991. Hamiltonian chaos and multi-fractal particle dynamics in 2D turbulence. *Modern Physics Letters A 6*, 83–91.

Osborne, A. R., Kirwan, A. D. Jr., Provenzale, A. and Bergamasco, L. 1986. A search for chaotic behaviour in large and measoscale motions in the Pacific Ocean. *Physica 23D*, 75–83.

Osborne, A. R., Kirwan, A. D. Jr., Provenzale, A. and Bergamasco, A. 1989. Fractal drifter trajectories in the Kuroshio extension. *Tellus 41A*, 416–435.

Osborne, A. R. and Provenzale, A. 1989. Finite correlation dimension for stochastic systems with power-law spectra. *Physica D35*, 357–381.

Ottino, J. M., Leong, C. W., Rising, H. and Swanson, P. D. 1988. Morphological structures produced by mixing in chaotic flows. *Nature 333*, 419–425.

Poulain, P. and Niiler, P. P. 1989. Statistical analysis of the surface circulation in the California current system using satellite-tracked drifters. *J. Phys. Oceanogr. 19*, 1588–1603.

Puri, S. C. and Mullen, K. 1980. *Applied statistics for food and agricultural scientists*. G. K. Hall Medical Publications, 311 pp.

Rapaport, D. C. 1985. The fractal nature of molecular trajectories in fluids. *J. Statistical Phys. 40*, 751–758.

Sanderson, B. G. 1982. *A Lagrangian description of drifter dispersion.* Ph.D. dissertation, Marine Sciences Research Center, State University of New York, Stony Brook, 197 pp.

Sanderson, B. G., Okubo, A. and Goulding, A. 1990. The fractal dimension of relative Lagrangian motion. *Tellus 42A*, 550–556.

Sanderson, B. G. and Pal, B. K. 1990. Patch diffusion computed from Lagrangian data, with application to the atlantic equatorial undercurrent. *Atmosphere-Ocean 28*, 444–465.

Taylor, G. I. 1921. Diffusion by continuous movements. *Proc. London Math. Soc. 20*, 196–211.

Thomson, R. O., LeBlond, P. H. and Emery, W. J. 1990. Analysis of deep-drogued satellite-tracked drifter measurements in the northeast Pacific. *Atmosphere-Ocean 28*, 409–443.